Bubble Rise Velocities and Drag Coefficients in Non-Newtonian Polysaccharide Solutions

Argyrios Margaritis, Derek W. te Bokkel, Dimitre G. Karamanev

Department of Chemical and Biochemical Engineering, The University of Western Ontario, London, Ontario, Canada N6A 5B9; telephone: (519) 661 2146; fax: (519) 661 3498; e-mail: amarg@julian.uwo.ca

Received 19 November 1998; accepted 15 March 1999

Abstract: Microbially produced polysaccharides have properties which are extremely useful in different applications. Polysaccharide producing fermentations start with liquid broths having Newtonian rheology and end as highly viscous non-Newtonian solutions. Since aerobic microorganisms are used to produce these polysaccharides, it is of great importance to know the mass transfer rate of oxygen from a rising air bubble to the liquid phase, where the microorganisms need the oxygen to grow. One of the most important parameters determining the oxygen transfer rate is the terminal rise velocity of air bubble. The dynamics of the rise of air bubbles in the aqueous solutions of different, mostly microbially produced polysaccharides was studied in this work. Solutions with a wide variety of polysaccharide concentrations and rheological properties were studied. The bubble sizes varied between 0.01 mm^3 and 10 cm^3. The terminal rise velocities as a function of air bubble volume were studied for 21 different polysaccharide solutions with different rheological properties. It was found that the terminal velocities reached a plateau at higher bubble volumes, and the value of the plateau was nearly constant, between 23 and 27 cm/s, for all solutions studied. The data were analyzed to produce the functional relationship between the drag coefficient and Reynolds number (drag curves). It was found out that all the experimental data obtained from 21 polysaccharide solutions (431 experimental points), can be represented by a new single drag curve. At low values of Reynolds numbers, below 1.0, this curve could be described by the modofoed Hadamard–Rybczynski model, while at Re > 60 the drag coefficient was a constant, equal to 0.95. The latter finding is similar to that observed for bubble rise in Newtonian liquids which was explained on the basis of the "solid bubble" approach. © 1999 John Wiley & Sons, Inc. *Biotechnol Bioeng* **64**: 257–266, 1999.
Keywords: non-Newtonian liquids; bubble; terminal velocity; drag coefficient; polysaccharides

INTRODUCTION

Biologically Produced Polysaccharides

Gas–liquid processes in which bubbles rise through a non-Newtonian liquid are of great importance to chemical and especially biochemical engineering. The knowledge of the fundamentals of hydrodynamics, and particularly the velocity of free rise of a single gas bubble in non-Newtonian liquid, is necessary for designing and operating efficiently many bioprocesses in pharmaceutical, environmental, and other industries.

Polysaccharides produced by fermentation are important sources of gums which are used in chemical, food, pharmaceutical, and other industries (Margaritis and Pace, 1986). Because of their unique properties, these gums are used as emulsifiers, stabilizers, binders, gelling agents, coagulants, lubricants, and thickening agents. Exopolysaccharides can be produced by many different species of bacteria, algae, and fungi (Margaritis and Zajic, 1978). Microbiologically produced by *Xanthomonas campestris* xanthan gum is presently the most popular exopolysaccharide. It has a large spectrum of applications and even larger future potential (Margaritis and Pace, 1986). Among other important exopolysaccharides are alginate produced by *Azotobacter vinelandii*, pullulan from *Aureobasidium pullulans*, and dextran produced by *Leuconostoc mesenteroides.*

During the fermentation process of exopolysaccharide production, the characteristics of the liquid media change drastically. While at the beginning the liquid has a Newtonian behavior with viscosity close to that of pure water, formation of exopolysaccharides results in the rapid increase in the apparent viscosity and change to non-Newtonian rheology. Since the processes of microbial production of polysaccharides are aerobic, the supply of the liquid media with oxygen during fermentation is of great importance. In the exopolysaccharide production, as in most other aerobic biotechnological processes, the oxygen is supplied by mass transfer between rising gas bubbles and liquid. The dynamics of bubble rise is one of the major parameters affecting the oxygen mass transfer rate from gas to liquid phase. Thus, to better understand and optimize the rate of oxygen transfer in the process of exopolysaccharide production, it is of fundamental importance to know the bubble rise dynamics in the fermentation broth.

Therefore, one of the major goals of this work is to study the dynamics of bubble rise in solutions of biologically produced exopolysaccharides.

Correspondence to: A. Margaritis
Contract grant sponsor: NSERC (Canada)

© 1999 John Wiley & Sons, Inc. CCC 0006-3592/99/030257-10

Bubble Rise Dynamics

Newtonian Fluids

The dynamics of bubble rise in Newtonian liquids has been an object of numerous studies. When gas bubble rise parameters were compared to these of free-falling heavy solid particle, significant differences were observed (Levich, 1962). This comparison was based on the presumption that free-falling heavy solid spheres behave exactly like freely rising light solid spheres.

Ever since Newton discovered the law of free settling, it has been universally assumed that the free rise of a buoyant particle should obey the laws of free settling of a heavy particle. This assumption seemed so obvious that no one proceeded to check it experimentally. However, experimental results reported recently (Karamanev and Nikolov, 1992) showed that the trajectory of free rising solid particles in Newtonian fluids was completely different compared to that of free falling particles, especially in the Newton's law region. In addition, the terminal velocity of rising particles was much lower than that of falling ones. The drag coefficient of free rising particles was constant at Reynolds numbers higher than 135 and was equal to 0.95, which is more than twice the value at the Newton's law region, describing the drag coefficients of falling particles (Karamanev, 1996). The difference between the free rise and free fall was explained by the effect of turbulence on the particle (Karamanev et al., 1996). However, the trajectories and terminal velocities of rising light rigid particles resembled those of gas bubbles (Karamanev, 1996).

This discovery led to the introduction of a new approach for the study of rising gas bubbles. It was named *solid bubble approach* and was based on the comparison in the behavior of a single gas bubble and a single rising light particle (solid bubble) with the same shape and size and with a similar density difference. The difference between the real and solid bubble dynamics can be used to reveal the effect of gas–liquid boundary motion and of bubble shape dilation on the bubble behavior. The application of solid bubble approach to bubble rise in Newtonian liquids resulted in the development of the first semianalytical equation describing the rise of a single gas bubble in quiescent Newtonian liquids over the entire range of Reynolds numbers (below the critical point) and bubble sizes and shapes (Karamanev, 1996).

Non-Newtonian Fluids

The most common among non-Newtonian fluids are the shear-thinning ones. While the power-law (two-parameter Ostwald de Waele) model is not the most precise among the available viscosity equations for this type of fluids (both Carreau (1972) and Ellis models describe the real situation better especially at very low and very high apparent viscosities), its simplicity is the main reason for its wide applicability (Chhabra, 1993). In this paper, we will study mainly shear-thinning fluids and will use the power-law model for their rheological description.

To calculate the bubble terminal velocity in non-Newtonian fluids, it is necessary to know the relationship between the drag coefficient of the gas bubble and Reynolds number (the drag curve). Since the fluid viscosity varies as a function of the shear rate, respectively particle terminal velocity, the first problem in developing the drag curve is the definition of Reynolds number since it contains both fluid viscosity and terminal velocity. One of the most commonly used forms of terminal Reynolds number is based on the assumption (Lali et al., 1989; Chhabra, 1986) that the average shear rate over the entire particle surface is equal to U_t/d_p. In this case, the apparent viscosity can be written as:

$$\mu_a = K\left(\frac{U_t}{d_p}\right)^{n-1}. \tag{1}$$

When this expression replaces viscosity in Reynolds number, the following form of Re for power-law fluids can be obtained for the case of a spherical particle:

$$Re_t = \frac{d_p^n U_t^{2-n} \rho}{K}. \tag{2}$$

According to Miyahara and Takahashi (1985) in the case of a nonspherical particle with a vertical axis of symmetry, the force balance showed that the Reynolds number should be expressed as:

$$Re_t = \frac{d_h^n U_t^{2-n} \rho}{K}. \tag{3}$$

The drag coefficient of a nonspherical particle with a vertical axial symmetry moving in either Newtonian or non-Newtonian fluid can be calculated on the basis of the force balance and is defined (Karamanev, 1994; Miyahara and Takahashi, 1985) as

$$C_D = \frac{4g\Delta\rho d_e^3}{3\rho d_h^2 U_t^2}, \tag{4}$$

where d_e is the equivalent sphere diameter and d_h is the diameter of the horizontal projection of bubble. In the above equation, the drag coefficient is calculated on the basis of the real bubble geometry (represented by d_h), while most other authors calculated it on the basis of the equivalent sphere diameter. The parameter d_h was calculated using the correlation of Wellek et al. (1966), as proposed by Clift et al. (1978).

Using Eqs. (2) and (3), Miyahara and Yamanaka (1993) showed that at Reynolds numbers below 10, the drag coefficient of bubbles rising in power-law liquids (CMC solutions with flow index between 0.63 and 0.86) can be described by the Hadamard–Rybczynsky (Hadamard, 1911; Rybczynsky, 1911) equation:

$$C_D = \frac{16}{Re_t}. \tag{5}$$

However, no universal drag curve has been proposed yet for the case of rising gas bubbles in non-Newtonian, and particularly, power-law fluids. One of the goals of this paper is to propose a drag curve, based on the relationship between C_D and Re (Eqs. (3) and (4)) for the rise of gas bubbles in power-law liquid with a wide range of rheological properties.

The main objectives of this work are:

- to study experimentally the dynamics of free bubble rise in non-Newtonian liquids typical for biotechnological polysaccharide production;
- to propose a correlation relating the drag coefficient and the terminal Reynolds number for air bubbles rising in power-law liquids with different rheological properties.

MATERIALS AND METHODS

Polysaccharide Solutions

Aqueous solutions of six different polysaccharides were used in this study: xanthan gum, sodium alginate, carboxymethylcellulose (CMC) as a sodium salt, low and high molecular weight dextran, and pullulan. Xanthan gum was obtained as a sample of Kelzan (Lot no. ZN16016A) from Charles Tennant and Co. The sodium salt of CMC was supplied by Hercules Inc. (type 9M31XF; Lot no. 46673). Na-alginate was obtained from Fisher Scientific Co. The low molecular weight dextran (MW 176,800) was supplied by Sigma Chemicals, as was high molecular weight dextran (MW 5×10^6–4×10^7). The pullulan used was produced using *A. pullulans* in the Department of Chemical and Biochemical Engineering of The University of Western Ontario by Drs. A. Margaritis and T. Jack. The microbial culture was grown on sucrose as a carbon source. The pullulan had been freeze-dried and stored before it was used in the present work.

The solutions were prepared by adding weighed amounts of the polysaccharides to distilled water. The homogenization was assured by mechanical mixing. Small 100-mL samples were used for the study of rheological and physical properties (flow and consistency index, density, and surface tension). Solutions were maintained at 23 ± 2°C during the experiments.

To obtain precise measurements of the bubble terminal velocity, the liquids used have to be transparent, so that laser beams can penetrate through them. From this point of view, there were problems with two of the polysaccharides used. The high MW dextran and pullulan were not transparent due to the presence of cell debris. They were clarified by centrifugation at 22,000*g* for 6–8 h, or at 8000*g* for 16–20 h.

Bubble Velocity Measurement

After a careful study of the available methods for the measurement of the terminal velocity of gas bubbles, we decided to use a twin-lased beam velocimeter. A schematic diagram of the velocimeter is shown in Fig. 1. The column was illuminated by two horizontal and parallel laser beams, passing through the axis of the column. The vertical distance between the beams was between 5.5 and 5.6 mm. Lenses were used to focus and produce a very fine laser beam of less than 10 μm in diameter. Two phototransistors (2N5777) on either side of the column intercepted the light beams from the lasers. A phototransistor-controlled, digital timer of ±5 μs/min accuracy was started and stopped by the sequential interruption of the laser beams resulting from the bubble rise. From the known distance between the laser beams and the calibrated timer reading, the rise velocity of the air bubble was calculated.

The lasers used were two 0.5-mW HeNe lasers, one supplied by C.W. Radiation (Model no. LS05R) and the other by Spectra Physics (Model no. 155).

The column was a rectangular plexiglass vessel with an internal size of 89 × 89 × 457 mm. The size of the column was large enough to avoid any wall effects (Chhabra, 1993; Chhabra and Uhlherr, 1980; Chhabra and Bangun, 1997).

Bubble Generation and Size Measurement

The bubble generation system consisted of either an orifice plate or a capillary tube for the release of gas bubbles. An air-fed inverted funnel was also used to produce the largest bubbles. The air was supplied from a compressor and was filtered. The air flow rate was adjusted so that bubbles were released once every 15 s or more. It has been shown that bubbles released at such intervals do not interact significantly with each other (Li et al., 1998). The bubble generator was centered in the column and the column position was adjusted so that the centre of the air bubble interrupted the laser beams.

Bubble volumes were determined using a photographic method. The bubbles were lit from behind using a 20-W

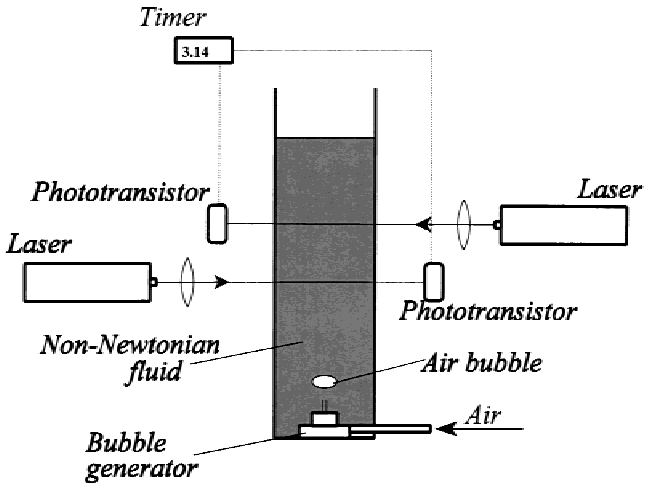

Figure 1. Schematic of the experimental apparatus used to measure terminal rise velocities.

fluorescent light source. A black and white photographic picture was taken from a distance of 250 mm from the laser beams. The bubbles were photographed as they crossed the laser beams. A millimeter scale in the tank was also photographed together with each bubble. The picture of the bubble was then digitized, and the bubble volume was calculated on the basis of the assumption that it had a vertical axis of symmetry. The volume of bubbles produced varied between 0.01 $mm^3$and 10 cm^3.

Determination of Physical Properties of Liquid

The rheological properties of the various polysaccharide solutions were studied using a Rotavisco (Haake Co.) viscometer. The measurements were performed at 25 ± 0.1°C. The readings were taken in both increasing and decreasing shear rates. Most of the measurements were performed at shear rates between 1 and 3000 s^{-1}. The shear rates during the rise of bubbles studied in this work were within the same range, except for the smallest bubbles in 2.91% CMC solution.

Surface tension was measured using a Fisher Autotensiostat equipped with a 50-mm du-Nouy ring. The elevator descent speed was normally set at 1.25 cm/min. Each solution was tested 5–10 times.

Density of liquid was determined using a glass pycnometer with a volume of 25 mL.

RESULTS AND DISCUSSION

Physicochemical Characteristics of Polysaccharide Solutions

The rheological behavior of non-Newtonian polysaccharide solution used (CMC, xanthan gum, Na-alginate, low and high molecular weight dextran, and pullulan) was studied by measuring the shear rate–shear stress relationship. Such a relationship for the case of pullulan solutions with different concentrations is shown in Fig. 2. Similar curves were obtained for all other non-Newtonian solutions used in this work. The linearity of the curves indicated that rheological characteristics of all the liquids studied under the experimental conditions of this work can be described by the power-law model. Values of the flow (n) and consistency (K) indices obtained are summarized in Table I.

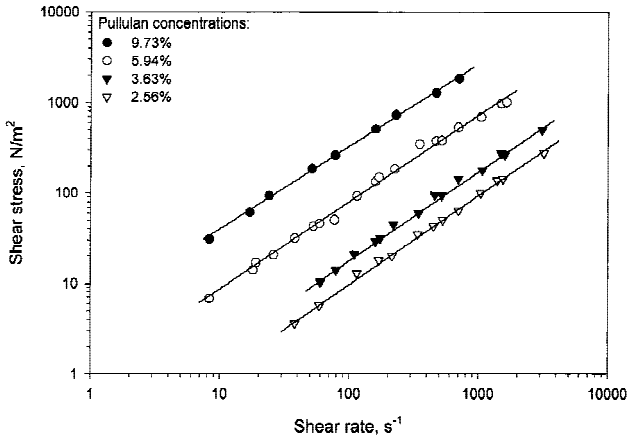

Figure 2. Shear rate–shear stress curve for pullulan solutions.

The effect of the polysaccharide concentration on the consistency index for the polysaccharides used is shown in Fig. 3. As expected, the consistency index approaches the pure water viscosity as the polysaccharide concentration approaches zero. At higher concentrations, the value of consistency index reached a plateau. A similar relationship was observed also by Thompson and Ollis (1980) and Chang and Ollis (1982).

In addition to the rheological properties, some other physicochemical parameters of the liquids studied were determined, such as density and surface tension.

It can be seen (Fig. 4) that density of most of the liquids used was similar to that of water when polysaccharide concentration was below 10 g/L. A significant density increase was observed as the concentrations were increased above 10 g/L, especially in the cases of both high and low molecular weight dextran as well as Na-alginate.

The surface tension of the solutions did not change significantly as a function of polysaccharides concentrations within the concentration ranges used in this study and remained close to that of water (72 g/cm^3).

Study of Bubble Rise Velocities

Terminal velocities of bubble rise were measured as a function of the bubble volume. Aqueous polysaccharide solutions with different concentrations, listed in Table I, were used as a liquid phase. In general, the bubble shapes observed in this study were similar to these reported earlier (Astarita and Apuzzo, 1965).

Carboxymethylcellulose

The volume–terminal velocity relationship for gas bubbles rising in carboxymethylcellulose solutions is shown in Fig. 5a. The bubble volumes were varied between 0.02 mm^3 and 10 cm^3. The shapes of the curves are similar to these reported by De Kee et al. (1986) and other authors. The terminal bubble velocity was proportional to the bubble volume in log scale at lower volumes, and reaches a plateau at high bubble volumes. The value of plateau terminal velocity was the same for liquids with different CMC concentrations having different rheological characteristics; it was equal to 24 cm/s. The terminal velocity of a bubble with given volume decreased as CMC concentration increased, due to the increase in the apparent liquid viscosity.

The drag curves of bubble rise in CMC solutions are presented in Fig. 5b. The drag coefficients were calculated using Eq. (4), while Reynolds numbers were calculated according to Eq. (3). It can be seen that drag coefficients of bubbles rising in solutions with different CMC concentra-

Table I. Rheological properties of solutions used.

Solution	Concentration (w/w%)	Flow index, n (dimensionless)	Consistency index, K (kg/m·s^{2-n})
Carboxymethylcellulose	0.100	0.942	0.0074
	0.374	0.874	0.0274
	0.695	0.804	0.0702
	0.744	0.800	0.118
	1.478	0.640	0.360
	1.961	0.559	2.04
	2.913	0.744	6.25
Xanthan gum	0.036	0.738	0.0130
	0.050	0.682	0.0239
	0.100	0.550	0.0867
	0.133	0.448	0.230
	0.374	0.322	1.08
	0.744	0.225	3.84
	1.478	0.262	7.73
	2.913	0.220	21.7
	4.762	0.160	43.4
Na-alginate	0.209	0.789	0.0393
	0.417	0.784	0.0873
	0.624	0.774	0.170
	1.241	0.605	1.93
	2.451	0.431	27.8
	4.762	0.389	263.0
Low MW dextran	2.439	0.964	0.0033
	4.762	0.984	0.0041
	9.091	0.841	0.0186
	13.04	0.982	0.0137
	16.67	0.988	0.0165
	23.08	0.976	0.0620
	28.57	0.990	0.0816
	37.50	1.053	0.387
	41.18	1.026	0.795
	44.44	1.000	1.39
	47.37	0.997	2.38
	50.00	1.002	3.72
High MW dextran	2.22	0.801	0.0695
	3.27	0.777	0.152
	4.88	0.760	0.335
	6.63	0.742	0.528
Pullulan	2.56	0.938	0.0147
	3.63	0.969	0.0224
	5.94	0.955	0.0971
	8.73	0.921	0.474

tions, and therefore, having different rheological characteristics, can be represented by a single line.

Xanthan Gum

Only a low range of concentrations (0.036–0.133%) could be used in these experiments because of the opacity of the liquid blocking the laser beams and making photography of the air bubbles difficult. It was found that most of the opacity was due to microbial cells debris. The effect of volume on terminal velocity of air bubbles rising in xanthan gum solutions is shown in Fig. 6a. It can be seen that the shapes of the curves are similar to these for CMC solutions. The mean plateau value of bubble terminal velocity was found to be equal to 27 cm/s, which is close to that for CMC.

Figure 6b shows the relationship between the drag coefficient (Eq. (4)) and Reynolds number (Eq. (3)) for gas bubbles rising in aqueous solutions of xanthan gum with different concentrations. The drag coefficient of bubbles rising in solutions with different concentrations, and therefore, different rheological characteristics, are very close to each other. Some dispersion can be observed however, at Reynolds numbers higher than 70.

Na-Alginate

Three different concentrations of this polysaccharide in water were studied. The opacity of the solution again limited the maximal Na-alginate concentration. Some hazing of the bubble photograph occurred, but bubble perimeters, and

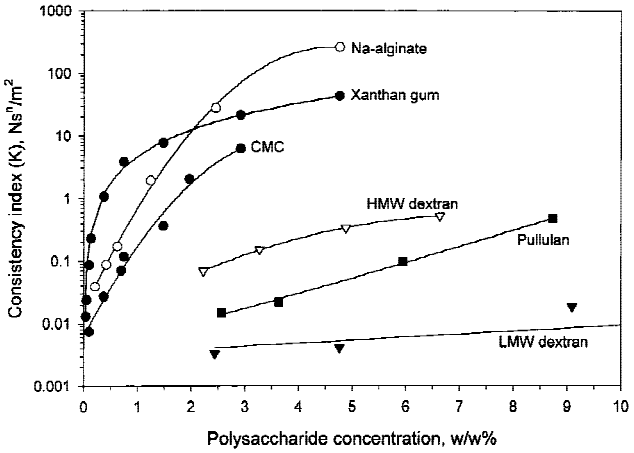

Figure 3. Effect of polysaccharide concentrations on their consistency index.

therefore bubble volume, could be determined with good precision. The velocity vs volume data for bubble rise in Na-alginate solutions is shown in Fig. 7a. The shapes of the curves were similar to these in the CMC and xanthan gum solutions. The plateau of bubble velocities was observed at 24 cm/s.

The drag curves for Na-alginate solutions are shown in Fig. 7b. Once again, the difference between the results with different polysaccharide concentrations were insignificant.

Low Molecular Weight (MW 176,800) Dextran

These solutions appear to display rheological behavior, close to that of Newtonian fluids since the flow index (n) is close to unity (Table I). The bubble volume–terminal velocity data are shown in Fig. 8a. The shapes of the experimental curves are similar to these obtained in the previous three experiments and also to the curve shapes obtained with contaminated Newtonian liquids. The value of plateau

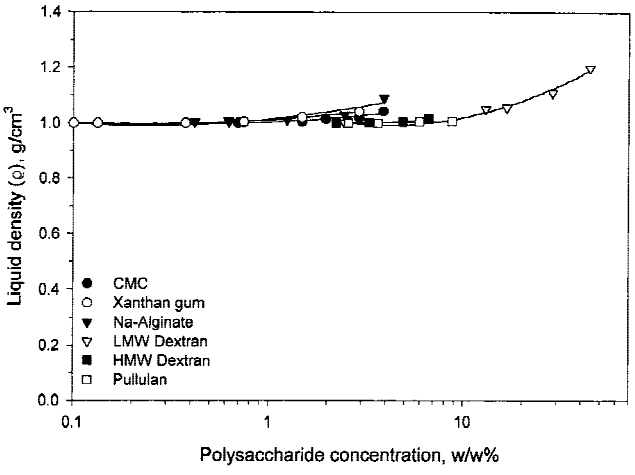

Figure 4. Effect of polysaccharides concentrations on the density of solutions.

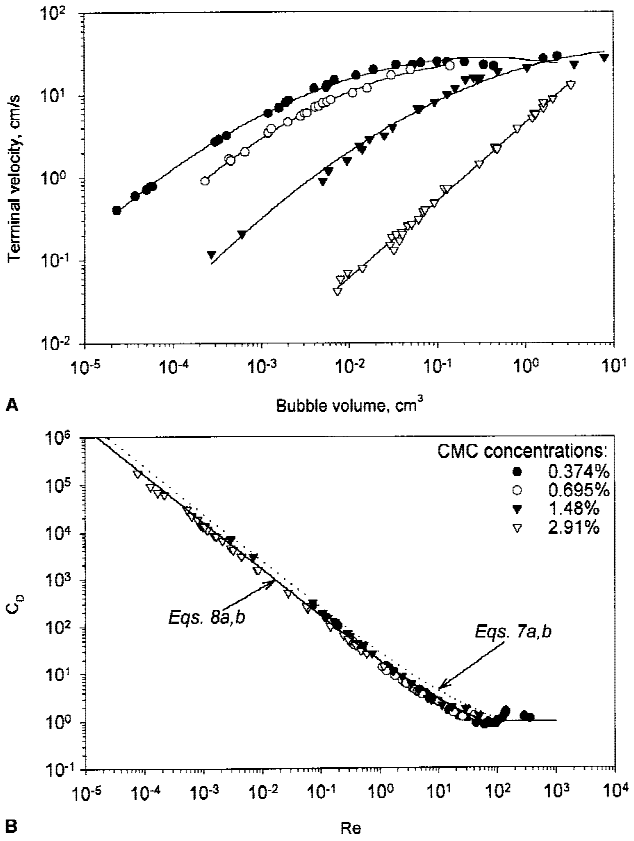

Figure 5. Terminal velocity curves bubble volume for CMC solutions (A). Drag coefficients of air bubbles versus Reynolds number for CMC solutions (B).

terminal velocity was found to be 26 cm/s. The drag curves of bubble rise in LMW dextran solutions are shown in Fig. 8b. The drag coefficient decreases as Re increases, and becomes constant at Reynolds numbers larger than 80.

High Molecular Weight (MW between 5 × 10^6 and 4 × 10^7) Dextran

These solutions were found to be non-Newtonian, since their flow indexes were well below unity (Table I). When all cellular debris was removed, these solutions proved to be translucent, and therefore, there were no problems in obtaining good quality photographic pictures. The terminal velocity–bubble volume data are shown in Fig. 9a. The plateau of bubble velocity was observed at 24 cm/s. The drag curves obtained for the different concentrations of polysaccharide were very consistent (Fig. 9b). The drag coefficient leveled again at Reynolds numbers higher than 70.

Pullulan Solutions

The natural dark brown pigment produced by *A. pullulans* could not be removed by centrifugation together with the microbial cell debris. This pigment caused problems with

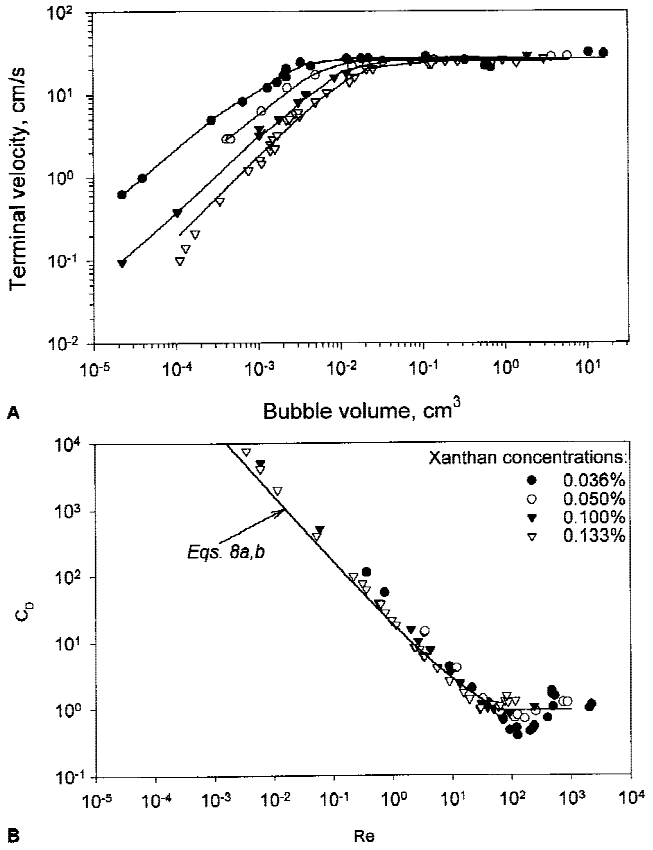

Figure 6. Terminal velocity curves bubble volume for xanthan gum solutions (A). Drag coefficients of air bubbles versus Reynolds number for xanthan gum solutions (B).

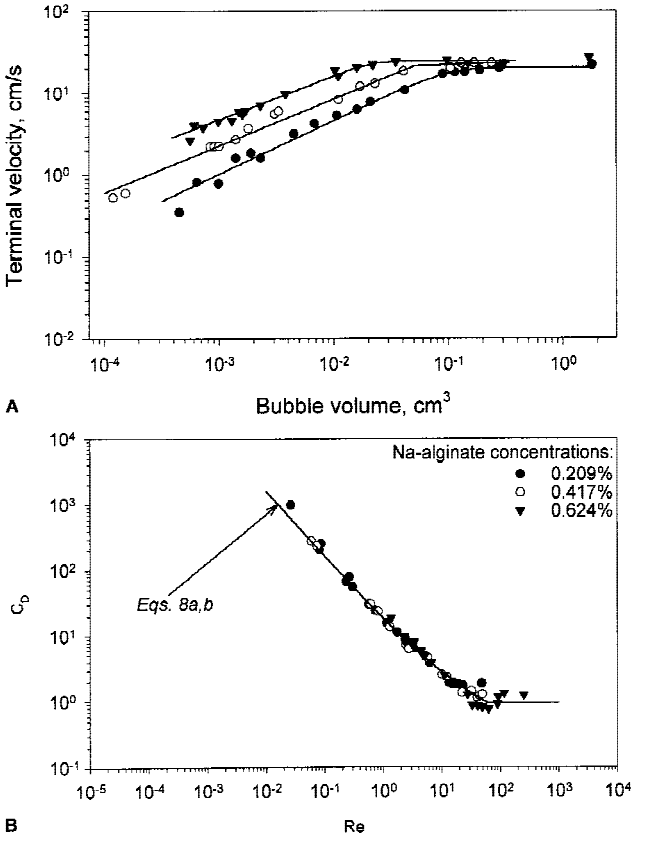

Figure 7. Terminal velocity curves bubble volume for Na-alginate solutions (A). Drag coefficients of air bubbles versus Reynolds number for Na-alginate solutions (B).

photography, and very small bubbles were very difficult to analyze because only a light smear appeared on the photographs. Although four concentrations of pullulan were initially studied, the lowest two were discarded due to the above mentioned problem. Figure 10a shows the terminal bubble rise velocity vs. bubble size for pullulan solutions. The plateau velocity was equal to 23 cm/s. The drag curves for the pullulan solutions are shown in Fig. 10b.

If one analyzes the results with different polysaccharides and different concentrations, it can be noted that all the velocity–volume curves have similar shapes. The relationship is linear at smaller bubble volumes (creeping flow of liquid), while it levels up when the bubble volume exceeds a certain value. The maximal (plateau) value of terminal velocity was between 23 and 27 cm/s in all the experiments, and therefore, was nearly constant. The slope of the logarithmic bubble volume–bubble velocity relationship under the liquid creeping flow conditions has been related to the flow index n by Astarita and Apuzzo (1965) by the following relationship:

$$\frac{1+n}{3n} = \frac{d \log U_t}{d \log V}. \tag{6}$$

The values of the flow index n obtained from the experimental slopes of the bubble volume–terminal velocity curves and Eq. (6) were compared to the experimental values determined by viscosimetry. The results are shown in Fig. 11. It can be seen that there is good agreement between the data, and therefore Eq. (6) describes well the situation at creeping flow regime.

Among the most interesting phenomena observed in the dynamics of bubble rise in non-Newtonian liquids is the bubble volume–terminal velocity curve discontinuity (Chhabra, 1988). It was observed by several authors, including Astarita and Apuzzo (1965), Acharya et al. (1977), Calderbank et al. (1970), and Rodrigue et al. (1996). The above-mentioned discontinuity is represented by a jump in the bubble terminal velocity when the bubble volume was increased over a certain limiting value. The jump can be by a factor of 10 (Chhabra, 1993). However, such a discontinuity was not observed at all by many other authors (Macedo and Yang, 1974; De Kee et al., 1986, 1990). In our study, a bubble volume–terminal velocity discontinuity was not observed in any of the experiments (Figs. 5a–10a).

Our next task was to develop an universal drag curve for bubble rise in power-law liquids. As it can be seen from Figs. 5b–10b, the drag coefficients calculated using Eq. (4) decreases as a function of Reynolds number (defined by Eq. (3)) until Re equals approximately 60 and after that level up. This shape is very similar to that of the drag curve of bubbles rising in contaminated Newtonian liquids (Kara-

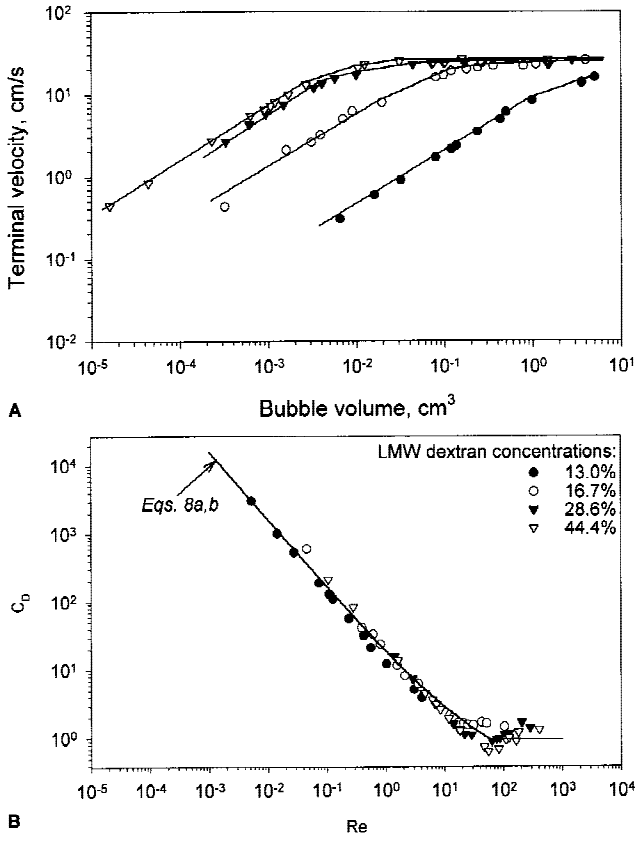

Figure 8. Terminal velocity curves bubble volume for low molecular weight dextran solutions (A). Drag coefficients of air bubbles versus Reynolds number for low molecular weight dextran solutions (B).

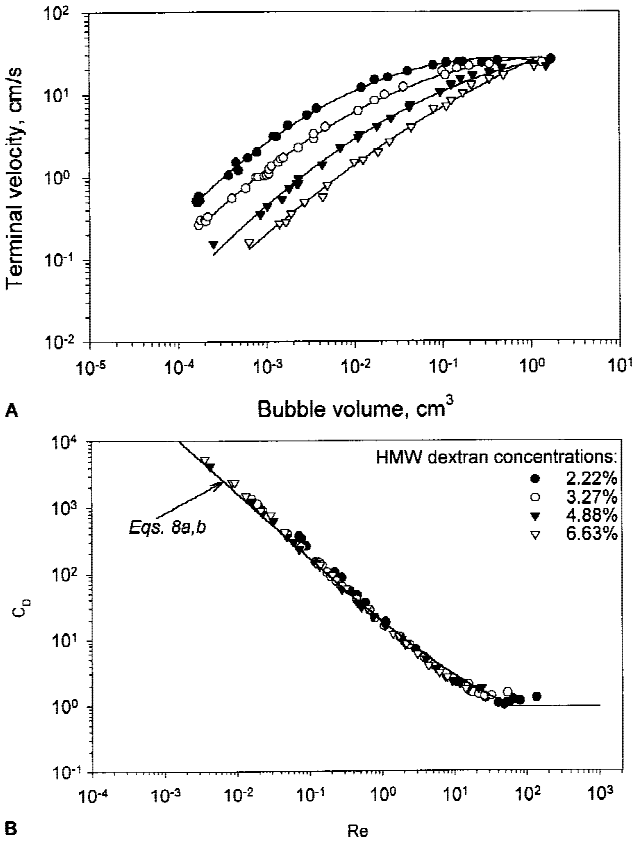

Figure 9. Terminal velocity curves bubble volume for high molecular weight dextran solutions (A). Drag coefficients of air bubbles versus Reynolds number for high molecular weight dextran solutions (B).

manev, 1996). The latter can be represented by the following correlation:

$$C_D = \frac{24}{Re_t}(1 + 0.173Re_t^{0.657}) + \frac{0.413}{1 + 16300Re_t^{-1.09}} \quad (7a)$$

for Re < 135, and

$$C_D = 0.95 \quad (7b)$$

for Re > 135.

When the curve representing Eqs. (7a) and (7b) was compared to the data for non-Newtonian liquids obtained in the present work, it was found that Eqs. (7a) and (7b) predicted higher values of C_D than the experimental values in almost the entire range of Re for any of the solutions used in this work. A comparison between Eqs. (7a) and (7b) and the experimental data with four different CMC solutions is shown in Fig. 5b. Similar results were obtained with all other polysaccharide solutions.

The drag curve for bubbles in contaminated Newtonian liquids (Eqs. (7a) and (7b)) was designed so that it converged to the Stokes equation ($C_D = 24/Re$) at small Reynolds numbers. However, it has already been shown (Miyahara and Yamanaka , 1993) that at low Reynolds numbers, the gas bubbles rising in power-law liquids obey not the Stokes but rather the Hadamard–Rybczynski model (Eq. (5)). Therefore, we modified Eq. (7a) so that it would converge to the Hadamard–Rybczynski model at small Reynolds numbers. This resulted in the following equation:

$$C_D = \frac{16}{Re}(1 + 0.173Re^{0.657}) + \frac{0.413}{1 + 16300Re^{-1.09}}. \quad (8a)$$

It can be seen from Figs. 5b–10b that, as in the case of gas bubbles in Newtonian liquids, the drag coefficient is close to a constant (0.95) at high Reynolds numbers. Since C_D in Eq. (8a) becomes equal to 0.95 at Re = 60, Eq. (8a) is valid only at Re < 60 while at Re > 60,

$$C_D = 0.95 \quad (8b)$$

This drag curve was compared to the experimental data reported in this study (Figs. 5b–10b). It can be seen that the new drag curve describes the experimental data quite well. Some scatter can be observed, however, at Reynolds numbers above 60 (plateau of the drag coefficient). This is probably due to the more turbulent conditions in this region. Similar scatter was observed also in the case of the move-

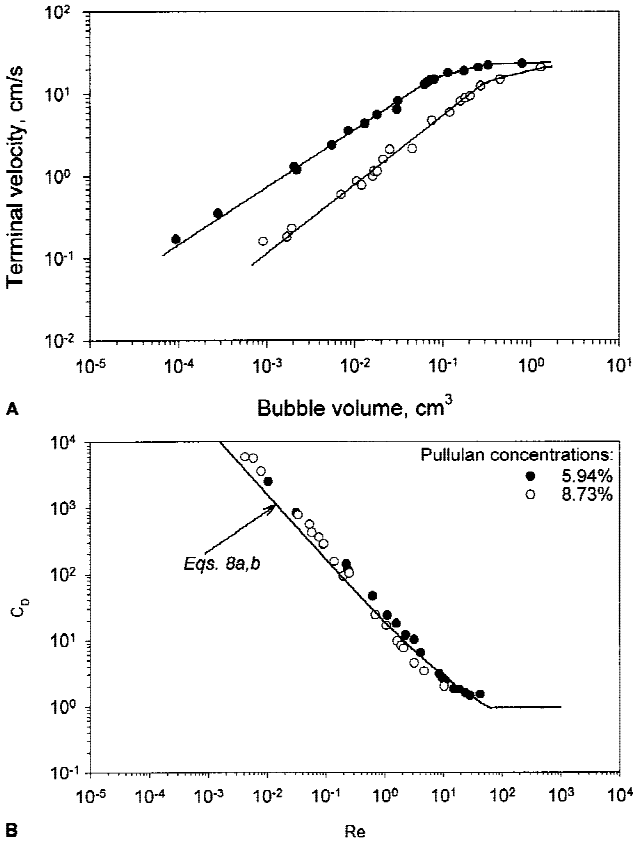

Figure 10. Terminal velocity curves bubble volume for pullulan solutions (A). Drag coefficients of air bubbles versus Reynolds number for pullulan solutions (B).

ment of both solid particles and bubbles in Newtonian liquids (Karamanev, 1996).

The drag curve in Fig. 12 is based on 431 experimental points obtained from six different non-Newtonian polysaccharide solutions with a total of 21 different concentrations. The fact that a single drag curve can describe the C_D–Re relationships for such a wide variety of non-Newtonian liquids with a broad range of rheological properties is very important for the practical determination of the bubble rise dynamics in such liquids. Moreover, most of the liquids used are actual biologically produced solutions of practical interest.

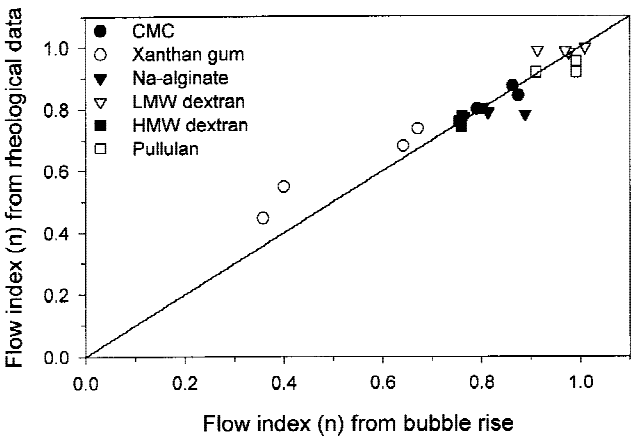

Figure 11. Comparison between the values of the flow index (n) obtained from rheological and bubble rise velocity data.

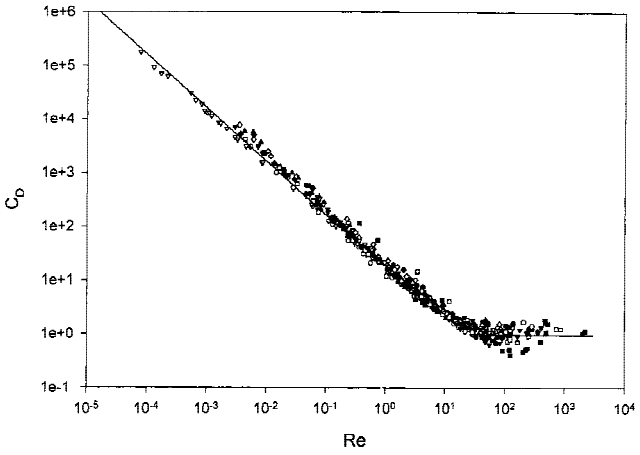

Figure 12. General correlation for all polysaccharide solutions studied.

NOMENCLATURE

C_D dragcoefficient
d_p spherical particle diameter, m
d_e diameter of volume-equivalent sphere, m
d_h horizontal bubble axis, m
g gravity acceleration, m/s^2
K consistency index, kg/(m·s^{2-n})
n flow index
Re_t terminal Reynolds number
U_t terminal velocity, m/s
V bubble volume, m^3

Greek letters

$\Delta\rho$ liquid–bubble density difference, kg/m^3
μ_a apparent viscosity, Pa.s
ρ liquid density, kg/m^3

This work was supported by the Natural Sciences and Engineering Research Council (NSERC) of Canada through an individual Research Grant awarded to Dr. A. Margaritis.

References

Acharya A, Mashelkar RA, Ulbrecht J. 1977. Mechanics of bubble motion and deformation in non-Newtonian media. Chem Eng Sci 32:863–872.

Astarita G, Apuzzo G. 1965. Motion of gas bubbles in non-Newtonian liquids. AIChE J 11:815–820.

Calderbank PH, Johnson DS, Loudon J. 1970. Mechanics and mass-transfer of single bubbles in free rise through some Newtonian and non-Newtonian liquids. Chem Eng Sci 25:235–256

Carreau PJ. 1972. Rheological equations from molecular network theories. Trans Soc Rheol 16:99–127.

Chang HT, Ollis DF. 1982. Extracellular microbial polysaccharides: Generalized power law for biopolysaccharide solutions. Biotechnol Bioeng 24:2309–2318.

Chhabra RP. 1986. Steady non-Newtonian flow about a rigid sphere. In:

Cheremisinoff NP, editor. Encyclopedia of fluid mechanics. Houston, TX: Gulf Publishers. Vol 1, p 983.
Chhabra RP. 1988. Hydrodynamics of bubbles and drops in rheologically complex liquids. In: Cheremisinoff NP, editor. Encyclopedia of fluid mechanics. Houston, TX: Gulf Publishers. Vol 7, p 253.
Chhabra RP. 1993. Bubbles, Drops and particles in non-Newtonian fluids. Ann Arbor, MI: CRC Press.
Chhabra RP, Uhlherr PHT. 1980. Wall effect for high Reynolds number motion of spheres in shear thinning liquids. Chem Eng Commun 5: 115–124.
Chhabra RP, Bangun J. 1997. Wall effects on terminal velocity of small drops in Newtonian and non-Newtonian fluids. Can J Chem Eng 75: 817–822.
Clift R, Grace JR, Weber ME. 1978. Bubbles, drops and particles. New York: Academic Press.
De Kee D, Carreau PJ, Mordarski J. 1986. Bubble velocity and coalescence in viscoelastic liquids. Chem Eng Sci 41:2273–2283.
De Kee D, Chhabra RP, Dajan A. 1990. Motion and coalescence of gas bubbles in non-Newtonian polymer solutions J Non-Newtonian Fluid Mech 37:1–18.
Hadamard JS. 1911. Mouvement permanent lent d'une sphère liquide et visqueuse dans un liquide visqueux. C R Acad Sci Paris 152: 1735–1738.
Karamanev DG. 1994. Rise of gas bubbles in quiescent liquids. AIChE J 40:1418–1421.
Karamanev DG. 1996. Equations for calculation of the terminal velocity and drag coefficient of solid spheres and gas bubbles. Chem Eng Commun 147:75–84.
Karamanev DG, Nikolov LN. 1992. Free rising spheres do not obey Newton's law for free settling. AIChE J 38:1993–1997.
Karamanev DG, Chavarie C, Mayer RC. 1996. Dynamics of the free rise of light solid sphere in liquid. AIChE J 42:1789–1792.
Lali AM, Khare AS, Joshi JB. 1989. Behaviour of solid particles in viscous non-Newtonian solutions: Settling velocity, wall effects and bed expansion in solid–liquid fluidized beds. Powder Technol. 57:39–50.
Levich VG. 1962. Physicochemical hydrodynamics. Englewood Cliffs, NJ: Prentice-Hall.
Li HZ, Mouline Y, Funfschilling D, Marchal P, Choplin L, Midoux N. 1998. Evidence for in-line bubble interactions in non-Newtonian fluids. Chem Eng Sci 53:2219–2230.
Macedo IC, Yang W-J. 1974. The drag of air bubbles rising in non-Newtonian liquids. Jpn J Appl Phys 13:529–533.
Margaritis A, Pace GW. 1986. Microbial polysaccharides. In: Cooney CL, Humphrey AE, editors. Comprehensive biotechnology: Principles, methods and applications. Oxford, UK: Pergamon Press. Vol 3, p 1005–1044.
Margaritis A, Zajic JE. 1978. Mixing, mass transfer and scale-up of polysaccharide fermentations. Biotechnol Bioeng 20:939–1001.
Miyahara T, Takahashi T. 1985. Drag coefficient of a single bubble rising through a quiescent liquid. Int Chem Eng 26:146–150.
Miyahara T, Yamanaka S. 1993. Mechanics of motion and deformation of a single bubble rising through quiescent highly viscous Newtonian and non-Newtonian media. J Chem Eng Jpn 26:297–302.
Rodrigue D, De Kee D, Chan Man Fong CF. 1996. An experimental study of the effect of surfactants on the free rise velocity of gas bubbles. J Non-Newtonian Fluid Mech 66:213–232.
Rybczynski W. 1911. Uber die fortschreitende bewegung einer flussigen kugel in einem zaben medium. Bull Acad Sci Cracow 1A:40–46.
Thompson N, Ollis DF. 1980. Extracellular microbial polysaccharides. II. Evolution of broth power-law parameters for xanthan and pullulan batch fermentations. Biotechnol Bioeng 22:875–883.
Wellek RM, Agrawal AK, Skelland AHP. 1966. Shape of liquid drops moving in liquid media. AIChE J 12:854.